

UNSTABLE DISK ACCRETION TO MAGNETIZED STARS: FIRST GLOBAL 3D MHD SIMULATIONS

MARINA M. ROMANOVA

Department of Astronomy, Cornell University, Ithaca, NY 14853-6801; romanova@astro.cornell.edu

AKSHAY K. KULKARNI

Department of Astronomy, Cornell University, Ithaca, NY 14853-6801; akshay@astro.cornell.edu

RICHARD V.E. LOVELACE

Department of Astronomy and Applied and Engineering Physics, Cornell University, Ithaca, NY 14853-6801; RVL1@cornell.edu

Subject headings: accretion, dipole — plasmas — magnetic fields — stars

Draft version November 8, 2018

ABSTRACT

We report on the first global three-dimensional (3D) MHD simulations of disk accretion onto a rotating magnetized star through the Rayleigh-Taylor instability. The star has a dipole field misaligned relative to the rotation axis by a small angle Θ . Simulations show that, depending on the accretion rate, a star may be in the stable or unstable regime of accretion. In the unstable regime, matter penetrates deep into the magnetosphere through several elongated “tongues” which deposit matter at random places on the surface of the star, leading to stochastic light-curves. In the stable regime, matter accretes in ordered funnel streams and the light-curves are almost periodic. A star may switch between these two regimes depending on the accretion rate and may thus show alternate episodes of ordered pulsations and stochastic light-curves. In the intermediate regime, both stochastic and ordered pulsations are observed. For $\Theta > 30^\circ$, the instability is suppressed and stable accretion through funnel streams dominates.

1. INTRODUCTION

Magnetospheric accretion occurs in different stars, for example in classical T Tauri stars (CTTSs), which are the progenitors of Solar-type stars (e.g., Hartmann 1998; Bouvier et al. 2007), in magnetized white dwarfs in some cataclysmic variables (e.g., Warner 1995; Warner & Woudt 2002), and in accreting millisecond pulsars, which are weakly magnetized neutron stars (e.g., van der Klis 2000). The matter close to the star may either flow around the magnetosphere, forming ordered funnel streams going towards the magnetic poles of the star (e.g., Ghosh & Lamb 1978; Camenzind 1990; Königl 1991), or may accrete directly through the magnetosphere due to the Rayleigh-Taylor (RT) instability (e.g., Arons & Lea 1976; Elsner & Lamb 1977; Scharlemann 1978). Earlier 2D and 3D numerical simulations have shown accretion through funnel streams (Koldoba et al. 2002; Romanova et al. 2002, 2003, 2004). Recent 3D MHD simulations performed for a *wider* range of parameters have shown that in many cases the disk-magnetosphere boundary is RT unstable.

Previous theoretical models and non-global simulations gave useful but restricted analyses of this problem. Arons and Lea (1976) investigated magnetospheric accretion through the RT instability in the non-rotating case with a spherical accretion geometry. Spruit and Taam (1990) investigated the stability of an infinitely thin rigidly rotating disk. The RT instability in magnetized disks was studied by Kaisig et al. (1992); Spruit et al. (1995); Lubow & Spruit (1995). Li and Narayan (2004) investigated disk-magnetosphere interaction in the case of an infinitely thick disk with a vertical magnetic field. 2D simulations have been performed by Wang and Nepveu (1983) and Wang & Robertson (1985), while Rastatter and Schindler (1999)

performed both 2D and 3D simulations, but in a patch (see also Stone and Gardiner 2007). Such simulations, while shedding light on many important features of the instability, do not take into account many factors which are present in global simulations, such as the possibility of matter flowing through funnel streams to the magnetic poles of the star.

In this paper we show results from global 3D MHD simulations, where the simulation region includes the disk and the whole magnetosphere of the star. This paper summarizes these new results, while in the following paper (Kulkarni & Romanova 2008, hereafter - KR08) we present results for a larger range of parameters.

2. MODEL AND RESULTS OF 3D MHD SIMULATIONS

2.1. Model. We use a “cubed sphere” Godunov-type numerical code (Koldoba et al. 2002) and solve the full set of 3D MHD equations with initial and boundary conditions similar to those used in Romanova et al. (2004). Simulations were done for non-relativistic as well as relativistic neutron stars. We approximate relativistic effects using the Paczynski-Wiita potential (Kulkarni & Romanova 2005). Our model includes viscosity to regulate the matter flux \dot{M} through the disk. The viscous stress in the disk is proportional to the α -parameter, which we varied in the range $\alpha = 0.02 - 0.3$. Most of the results shown here are for the grid $N_r \times N_x \times N_y = 148 \times 61 \times 61$ in each of the 6 blocks of the “cubed sphere”. Test simulations for twice as fine a grid and twice as coarse a grid show that the number of modes does not depend on the grid resolution.

The simulations are done in dimensionless form and are applicable to stars over a wide range of scales, if the magnetospheric radius r_m is not very large compared to the radius of the star R_* , $r_m = (4-5)R_*$; r_m is determined by

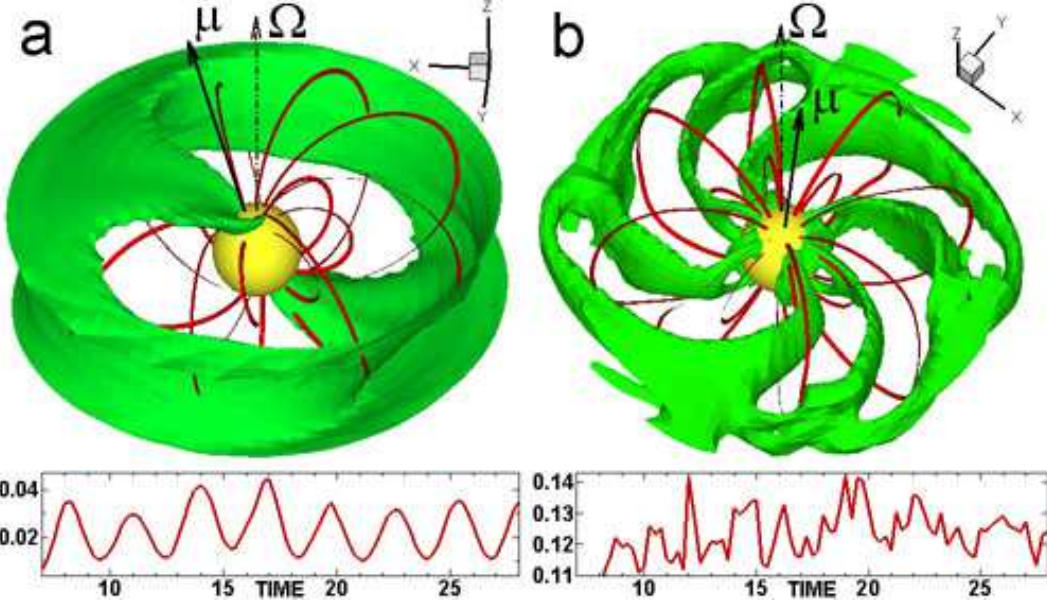


FIG. 1.— (a) An example of stable accretion. The surface is a constant density surface, and the lines are sample magnetic field lines. The magnetic axis is misaligned relative to the rotational axis by $\Theta = 15^\circ$. (b) An example of unstable accretion for $\Theta = 5^\circ$. The lower panels show light curves from the hot spots. Time is measured in orbital periods at $r = 1$. Only the inner part of the simulation region is shown.

the balance between the magnetospheric and matter pressure, so that the modified plasma parameter at the disk-magnetosphere boundary $\beta = (p + \rho v^2)/(B^2/8\pi) \approx 1$. The reference units are as follows: the length $R_0 = R_*/0.35$, velocity $v_0 = (GM_*/R_0)^{1/2}$, period $P_0 = 2\pi R_0/v_0$, density $\rho_0 = B_0^2/v_0^2$, magnetic moment $\mu_0 = B_0 R_0^3$, accretion rate $\dot{M}_0 = \rho_0 v_0 R_0^2$ (see KR08 for a complete description of units). We show results for a star with a dimensionless magnetic moment $\mu = 2$. We varied the period P_* of the star so that the corotation radius $r_{cor} = (GM/\Omega_*^2)^{1/3}$ in dimensionless units varied in the range $r_{cor} = 1.2 - 3$ (with $r_{cor} \approx 2$ in the main case). The initial disk structure is determined by the initial disk-corona-magnetic field equilibrium (e.g., Romanova et al. 2002) and it has the same fiducial density in all runs, so that the accretion rate in the disk is regulated mainly by the α -parameter of viscosity. The disk is sufficiently large ($R_d \approx 48R_*$) to supply matter during the whole simulation run, which lasted up to 50 periods of rotation P_0 . Most of the runs performed were for the small misalignment angle $\Theta = 5^\circ$ which helps excite the perturbations. Runs for larger Θ have shown that the instability is present up to $\Theta \approx 30^\circ$ (see KR08).

2.2. Stable and unstable regimes of accretion. In our earlier work we performed 3D MHD simulations of the disk-magnetosphere interaction for a variety of misalignment angles from $\Theta = 0^\circ$ to $\Theta = 90^\circ$, and showed that matter flows from the inner regions of the disk to the star in symmetric funnel streams, which are quasi-stable features over long times (Romanova et al. 2003, 2004). Figure 1a shows an example of accretion through funnel streams for $\Theta = 15^\circ$. In this type of flow, matter is lifted above the equatorial plane and then flows along field lines. The streams hit the star near the magnetic poles, forming ordered hot spots.

Next we chose a case with a small misalignment angle ($\Theta = 5^\circ$) and increased the accretion rate in the disk, increasing the α -parameter. We observed that at a critical value of $\alpha = 0.04$, the instability appears and the accretion acquires an essentially different pattern: the RT instability develops at the inner edge of the disk, and matter accretes through equatorial “tongues” which penetrate deep into the magnetosphere. The structure of the tongues is opposite to that of the funnel streams: they are narrow and tall (see Figure 1b). Such a tongue shape is determined by the geometry of the magnetic field and has been predicted by Arons and Lea (1976). Simulations performed for different parameters and grid resolutions have shown that the number of growing modes is always small, $m = 2 - 7$ (KR08). The matter energy-density dominates inside these tongues. Test runs at twice as large density in the disk have shown that the instability appears even at $\alpha = 0.02$ which proves that the matter accretion rate, and not α , is important. During the interchange process, the heavy fluid elements of the disk (matter dominated) change positions with the light fluid elements of the magnetosphere (magnetically-dominated). The magnetospheric plasma carries frozen-in magnetic field lines, so that displacing the light fluid leads to the effect of pushing magnetic field lines aside (see Figure 2). Equatorial slices of the density distribution for two moments of time are shown in Figure 3 (see also <http://astro.cornell.edu/us-rus/stereo.htm> for animations).

2.3. Light-curves from the hot spots on the surface of the star were calculated, to study the difference in observational properties between the stable and unstable regimes. We assume that the kinetic energy of the stream is converted at the surface of the star into isotropic black-body radiation. Integration of radiation in the direction of the

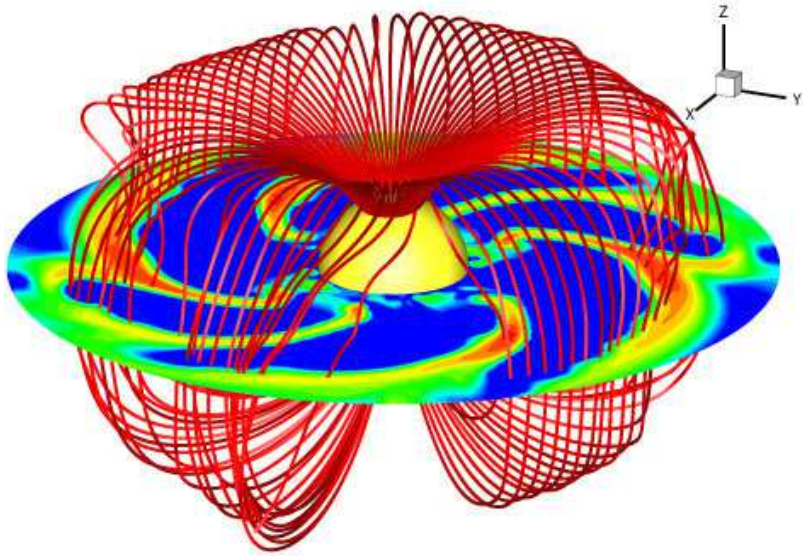


FIG. 2.— Penetration of the tongues through the magnetosphere. The tongues are shown by density contours in the equatorial plane (the highest density is shown in red, and the lowest in dark-blue, with a density contrast of about 300).

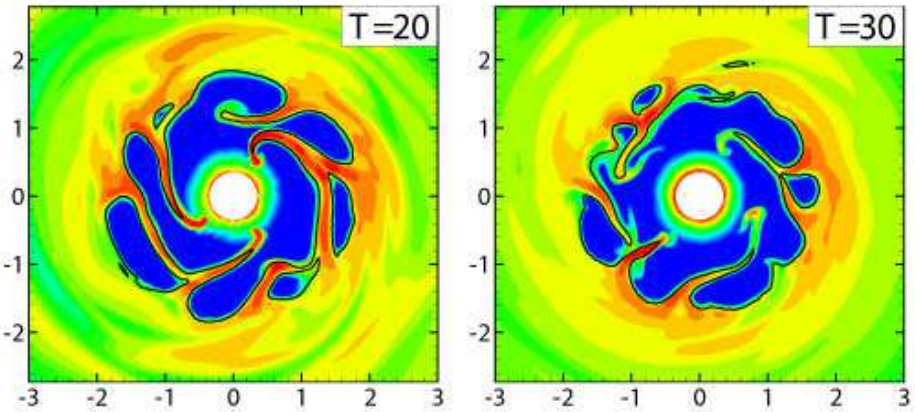


FIG. 3.— Density distribution in the equatorial plane after 20 and 30 periods of rotation at $r = 1$. The background shows the density (the colors have the same meaning as in Figure 2). The black line shows the position of $\beta = 1$. The plots are shown in the reference frame rotating with the star.

observer is performed (see details in R04). In the stable regime, the position of the hot spots is almost constant, so that the light-curve is almost sinusoidal (see Figure 1a, bottom panel). In the strongly unstable regime, sporadically forming tongues hit the star in random places, so that the light curve is irregular (see Figure 1b, bottom panel). In the intermediate cases both funnels and tongues are present, and mixed light-curves are expected. If a certain number of tongues dominates (for example, the $m = 2$ mode dominates in some cases) then quasi-periodic oscillations are expected. A more detailed analysis of the light-curves in different cases will be presented in a future paper.

2.4. Onset of instability. We compared our simulations with a few relevant theoretical approaches. A heavy fluid supported against gravity by a lighter one is RT unstable unless there is some opposing force. A homogeneous vertical field at the disk-magnetosphere boundary does not oppose the growth of ϕ -modes (see e.g. Chan-

drasekhar 1961). A more general criterion for differentially rotating magnetized accretion disks indicates that the disk is unstable to excitation of ϕ -modes if $\gamma_{B\Sigma}^2 \equiv -g_{eff}d\ln(\Sigma/B_z)/dr > 2(r_m d\Omega/dr)^2 \equiv \gamma_\Omega^2$ (Spruit et al. 1995; Spruit & Taam 1990; Kaisig et al. 1992; Lubow & Spruit 1995). Here, $-g_{eff} = r(\Omega_K^2 - \Omega^2)$ is the effective gravity, and $\Sigma = 2\rho h$ is the surface density. That is, for the instability to start, the surface density per unit magnetic field strength Σ/B_z should drop off fast enough in the direction of the effective gravity ($-g_{eff}$), so that the term $\gamma_{B\Sigma}^2$ is larger than the term associated with the shear, γ_Ω^2 , which tends to oppose the instability by smearing out the perturbations. We calculated the ϕ -averaged values of $\gamma_{B\Sigma}^2$ and γ_Ω^2 for the stable and unstable cases (see Figure 4) and compared the positions of the curves in the inner regions of the disk where the instability starts, that is at $r \gtrsim r_m$. One can see that in the stable case ($\alpha = 0.02$), $\gamma_{B\Sigma}^2 \lesssim \gamma_\Omega^2$ while in the unstable case ($\alpha = 0.1$) $\gamma_{B\Sigma}^2 \gg \gamma_\Omega^2$. Thus the theory makes a reasonably good prediction for the onset of

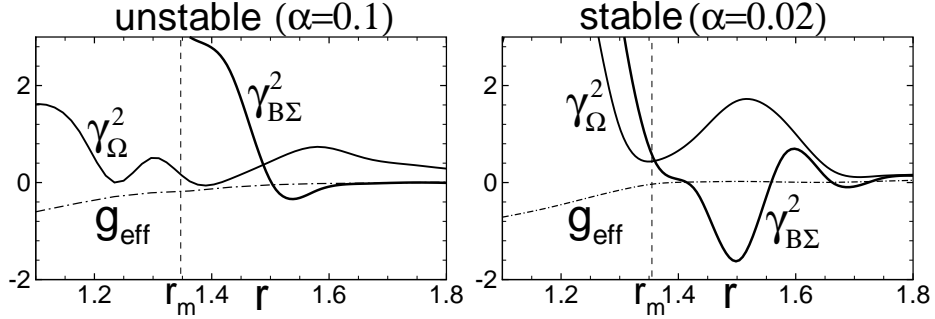


FIG. 4.— Parameters corresponding to the stability criterion by Spruit et al. (1995) described in §2.4.

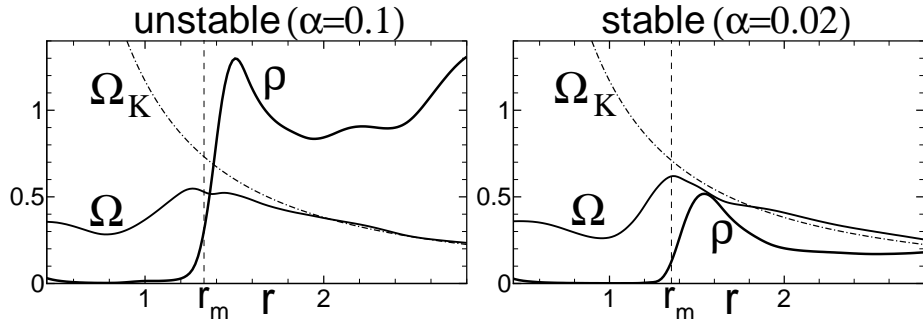


FIG. 5.— Radial distribution of the density ρ , angular velocity Ω and Keplerian angular velocity Ω_K in the equatorial plane. The dashed line r_m marks the position of the magnetospheric radius where $\beta = 1$.

instability. The term $\gamma_{B\Sigma}^2$ varies strongly mainly because in the unstable case, a significant amount of matter accumulates near r_m and the density drop-off is sharper than in the stable case (see Figure 5).

The RT modes observed in simulations are excited by different mechanisms. One of them is the small non-axisymmetry associated with the misalignment of the dipole. Another is the inhomogeneities in the inner regions of the disk driven by the azimuthal component of the field trapped inside the inner regions of the disk. The Kelvin-Helmholtz instability seems to be less significant (see also Rastatter & Schindler 1999).

2.5. Why low- m modes dominate. According to the theory of the RT instability, high- m modes should grow faster than low- m ones (e.g. Chandrasekhar 1961). In a rotating disk, the shear $d\Omega/dr$ may efficiently damp high- m modes (e.g., Lubow & Spruit 1995) and may be the main reason for damping of the high- m modes in our simulations. Initially, in high-resolution simulations we see the formation of $m = 20 - 30$ modes, but in one rotation period they are damped, and only the low- m modes grow. KR08 analyzed the number of modes based on the Li & Narayan (2004) criterion and reached a similar conclusion.

Another possible reason for the suppression of the high- m modes is the presence of the azimuthal component B_ϕ of the field at the inner edge of the disk which typically constitutes $\sim (5-30)\%$ of the poloidal component. The damping effect of B_ϕ is expected from theory (Chandrasekhar 1961), and has been noticed by Wang & Nepveu (1983) and Rastatter & Schindler (1999).

2.6. Boundary between the stable and unstable regimes. We performed multiple simulation runs for identical initial density distributions in the disk but different

viscosity parameters α and dimensionless periods of the star P_*^{dim} (these bulk simulations were done for a grid 72×31^2). The symbols in Figure 6a correspond to different runs. One can see that there is a boundary between the stable and unstable cases with unstable cases corresponding to higher α . For similar initial disks and accretion rates through the disks, \dot{M} is proportional to α , and thus the instability occurs at high enough accretion rates through the disk. The boundary is higher at smaller periods P_*^{dim} , because at faster rotation of the star the effective gravity becomes less negative and thus less matter may accumulate at the inner edge of the disk. That is why a larger α is required to bring more matter to the inner edge of the disk to satisfy the instability criterion. Cases with periods $P_*^{dim} \approx 2.7 - 3$ correspond approximately to the rotational equilibrium state (Long et al. 2005). Stars with smaller periods spin down and, at $P_*^{dim} \lesssim 1.8$, enter the “propeller” regime, where $r_{cor} < r_m$ (e.g. Illarionov & Sunyaev 1975; Lovelace et al. 1999; Rappaport et al. 2004). In this regime a star tends to expel a significant part of incoming matter (Romanova et al. 2005; Ustyugova et al. 2006). At high enough α we observed events of instability even in this regime (see also Wang & Robertson 1985), but the simulation runs were brief, and this region requires further analysis.

We calculated the accretion rate onto the surface of the star \dot{M}_*^{dim} for the above runs. The boundary between stable and unstable accretion $\dot{M}_*^{dim} \approx 0.3$ seems to be almost independent of P_* , which is probably a result of the combination of the lower disk density due to the propeller effect, and higher α . This boundary is approximate, with intermediate cases above and below it in which only marginal

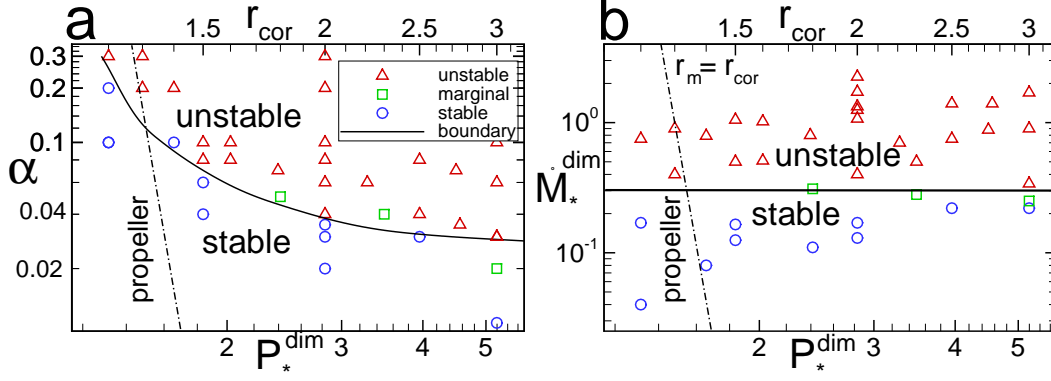


FIG. 6.— Position of stable (circles), unstable (triangles) and marginal (squares) cases in the (a) α - P_*^{dim} and (b) \dot{M}_*^{dim} - P_*^{dim} planes. The top horizontal axis shows the corotation radius. The solid lines show an approximate boundary between stable (below) and unstable (above) runs. The dash-dotted line marks the approximate boundary of the propeller regime.

instability is observed. In this transition region, both funnels and tongues are present. Higher up, for $\dot{M}_*^{\text{dim}} > 0.5$, the instability is strong and accretion through tongues dominates. We note that at low enough accretion rates through the disk even stable accretion may shut-off, because there is insufficient pressure gradient at the disk-magnetosphere boundary to form magnetospheric funnel streams.

2.7. Application to different magnetized stars. The results of our simulations can be applied to a variety of magnetized stars with small magnetospheres, $r_m \approx (4 - 5)R_*$, including CTTSs, weakly magnetized white dwarfs (WDs) in cataclysmic variables and neutron stars (NSs) in LMXBs. The dividing line in Figure 6b corresponds to $\dot{M}_*^{\text{dim}} \approx 0.3$. Below we show the accretion rate corresponding to this boundary in dimensional units for different types of stars:

$$\text{CTTSs : } \dot{M}_*^{\text{cr}} \approx 2.1 \times 10^{-8} (B_*/10^3 \text{G})^2 r^{\frac{5}{2}} m^{-\frac{1}{2}} M_\odot/\text{yr},$$

$$\text{WDs : } \dot{M}_*^{\text{cr}} \approx 1.4 \times 10^{-8} (B_*/10^6 \text{G})^2 r^{\frac{5}{2}} m^{-\frac{1}{2}} M_\odot/\text{yr},$$

$$\text{NSs : } \dot{M}_*^{\text{cr}} \approx 2.2 \times 10^{-9} (B_*/10^9 \text{G})^2 r^{\frac{5}{2}} m^{-\frac{1}{2}} M_\odot/\text{yr}.$$

The period in dimensional units is:

$$P_* = A_p P_*^{\text{dim}} m^{-\frac{1}{2}} r^{\frac{3}{2}},$$

where scaling factors for different stars are:

CTTSs: $A_p \approx 1.78$ days, $r = R_*/2R_\odot$, $m = M_*/0.8M_\odot$,

WDs: $A_p \approx 29.4$ sec, $r = R_*/5 \times 10^8$ cm, $m = M_*/1M_\odot$,

NSs: $A_p \approx 2.22$ ms, $r = R_*/10^6$ cm, $m = M_*/1.4M_\odot$.

Note that the dimensional \dot{M}_*^{cr} increases with the magnetic field as B_*^2 so that the boundary will be higher for higher B_* . This reflects the fact that we have fixed the dimensionless magnetic moment μ , and thus consider stars with an approximately fixed ratio $r_m/R_* \approx 4 - 5$. We performed another set of runs for smaller magnetospheres (smaller r_m/R_* for $\mu = 0.5$) and observed that the dimensionless boundary corresponds to a smaller \dot{M}_*^{dim} (see

KR08). Note also that all the above runs were done for $\Theta = 5^\circ$. We expect that for larger Θ the boundary will move up, because funnel accretion is more favorable at larger Θ .

3. OBSERVATIONAL CONSEQUENCES

The existence of two regimes of accretion changes our understanding of accreting magnetized stars and their observational properties: the lack of a periodic signal in the light curve does not rule out accretion and an ordered magnetic field. For example, the random light-curves in many CTTSs or dwarf novae do not preclude an ordered stellar field, if the star is in the unstable regime. Depending on the accretion rate, episodes of stable and unstable accretion may alternate, so that periods with pulsations may be *intermittent* and may be followed by periods with no pulsations. Recently a number of intermittent accreting millisecond pulsars have been discovered (e.g., Kaaret et al. 2006; Altamirano et al. 2007; Galloway et al. 2007; Gavriil et al. 2007). Although the reason for this behavior is not yet understood, we note that in, for example, HETE J1900.1–2455, the pulsations disappeared when the overall X-ray flux increased (Kaaret et al. 2006) which may be an example of a transition to the unstable accretion regime.

In some cases a definite number of tongues may dominate, which may lead to quasi-periodic oscillations in the light curves (Li & Narayan 2004). These oscillations may be candidates for one of the QPOs observed in Type II (accretion-driven) bursts in LMXBs. Comptonization of photons by high-energy electrons may lead to only a small departure of the light-curve from the thermal ones obtained using the approximation of isotropic black-body radiation (Poutanen & Gierliński 2003), so that the QPO features may survive Comptonization (see, however, Titarchuk et al. 2007).

In the case of young stars surrounded by gas/dust disks where planets are forming and migrating inward, the unstable tongues may support inward migration, so that the magnetospheric gap, which can halt migration (e.g. Lin et al. 1996; Romanova & Lovelace 2006; Papaloizou 2007), may form only in the state of stable accretion.

We thank the anonymous referee for valuable suggestions which improved the paper. We thank Drs. A.

Koldoba and G. Ustyugova for their contribution to the code development and Drs. D. Altamirano, L. Hillenbrand, P. Kaaret, and C. Thompson for discussions. NASA provided high-performance computational facilities

for this work. The research was partially supported by the NSF grants AST-0507760 and AST-0607135, and the NASA grants NNG05GG77G and NNG05GL49G.

REFERENCES

Altamirano, D., Casella, P., Patruno, A., Wijnands, R., van der Klis, M. 2007, astro-ph: 0708.1316

Arons, J. & Lea, S. M. 1976, ApJ, 207, 914

Bouvier, J., Alencar, S. H. P., Harries, T. J., Johns-Krull, C. M. & Romanova, M. M. 2007, *Protostars and Planets V*, B. Reipurth, D. Jewitt, and K. Keil (eds.), University of Arizona Press, Tucson, 479

Camenzind, M. 1990, Rev. Mod. Astron. 3, 234

Chandrasekhar, S. 1961, *Hydrodynamic and hydromagnetic stability*. Oxford Univ. Press: London

Elsner, R.F. & Lamb, F.K. 1977, ApJ, 215, 897

Galloway, D.K., Morgan, E.H., Krauss, M.I., Kaaret, P., Chakrabarty, D. 2007, ApJ, 654, L73

Gavriil, F.P., Strohmayer, T. E., Swank, J. H., Markwardt, C.B. 2007, ApJ, 669, L29

Ghosh, P. & Lamb, F. K. 1978, ApJ, 223, L83

Hartmann, L. 1998, *Accretion processes in star formation*. Cambridge: Cambridge Univ. Press.

Illarionov, A.F., & Sunyaev, R.A. 1975, A&A, 39, 185

Kaaret, P., Morgan, E.H., Vanderspek, R., Tomsick, J.A. 2006, ApJ, 638, 967

Kaisig, M., Tajima, T., & Lovelace, R. V. E. 1992, ApJ, 386, 83

Koldoba, A.V., Romanova, M. M., Ustyugova, G. V. & Lovelace, R. V. E. 2002, ApJ, 576, L53

Königl, A. 1991, ApJ, 370, L39

Kulkarni, A.K. & Romanova, M.M. 2005, ApJ, 633, 349

Kulkarni, A.K. & Romanova, M.M. 2008, MNRAS, in press

Li, L.-X. & Narayan, R. 2004, ApJ, 601, 414

Lin, D. N. C., Bodenheimer, P. & Richardson, D. C. 1996, Nature, 380, 606

Long, M., Romanova, M.M. & Lovelace, R.V.E. 2007, MNRAS, 374, 436

Lovelace, R.V.E., Romanova, M.M. & Bisnovatyi-Kogan, G.S. 1999, ApJ, 514, 368

Lubow, S.H., & Spruit, H.C. 1995, ApJ, 445, 337

Papaloizou, J. C. B. 2007, A&A, 463, 775

Poutanen, J., & Gierlinski, M. 2003, MNRAS, 343, 1301

Rappaport, S.A., Fregeau, J.M. & Spruit, H. 2004, ApJ, 606, 436

Rastatter, L. & Schindler, K. 1999, ApJ, 524, 361

Romanova, M. M. & Lovelace, R. V. E. 2006, ApJ, 645, L73

Romanova, M.M., Ustyugova, G.V., Koldoba, A.V., Wick, J.V., & Lovelace, R.V.E. 2003, ApJ, 595, 1009

Romanova, M. M., Ustyugova, G. V., Koldoba, A. V. & Lovelace, R. V. E. 2004, ApJ, 610, 920

Romanova, M. M., Ustyugova, G. V., Koldoba, A. V. & Lovelace, R. V. E. 2005, ApJ, 616, L165

Scharlemann, E.T. 1978, ApJ, 219, 617

Spruit, H. C., Stehle, R., & Papaloizou, J.C.B. 1995, A&A, 229, 475

Spruit, H. C. & Taam, R. E. 1990, A&A, 229, 475

Stone, J.M. & Gardiner, T. 2007, astro-ph 0709.0452

Titarchuk, L., Kuznetsov, S., & Shaposhnikov, N. 2007, astro-ph 0706.1595

Ustyugova, G.V., Koldoba, A.V., Romanova, M.M., & Lovelace, R.V.E. 2006, ApJ, 646, 304

Van der Klis, M. 2000, Annu. Rev. Astron. Astrophys. 38, 717

Wang, Y.-M. & Nepveu, M. 1983, A&A, 118, 267

Wang, Y.-M. & Robertson, J. A. 1985, ApJ, 299, 85

Warner, B. 1995, *Cataclysmic variable stars*. Cambridge Astrophysics Series, Cambridge, New York: Cambridge University Press

Warner, B. & Woudt, P.A. 2002, MNRAS, 335, 84